

## Quantum tomography of a laser beam interacting with cold atoms

T. COUDREAU<sup>1</sup>, L. VERNAC<sup>1</sup>, A. Z. KHOURY<sup>1</sup>(\*)  
G. BREITENBACH<sup>2</sup> and E. GIACOBINO<sup>1</sup>

<sup>1</sup> *Laboratoire Kastler-Brossel (\*\*), Case 74, UPMC*

*4 Place Jussieu 75252 Paris Cedex 05, France*

<sup>2</sup> *Fakultat für Physik, Universität Konstanz - D78434, Konstanz, Germany*

(received 23 December 1998; accepted in final form 16 April 1999)

PACS. 32.80Pj – Optical cooling of atoms; trapping.

PACS. 42.50Lc – Quantum fluctuations, quantum noise, and quantum jumps.

PACS. 42.50Ar – Photon statistics and coherence theory.

**Abstract.** – We have used the method of quantum tomography to reconstruct the Wigner function of squeezed light generated from a laser beam having interacted with cold atoms. The photon number distribution has been investigated showing features of squeezed states.

All knowable information about a quantum state is given by its density matrix,  $\rho$ , or by its Wigner function,  $W$ . The Wigner function is a quasi-probability distribution [1] and allows to calculate all expectation values of any symmetrized product of operators. Thus, the reconstruction of the Wigner function from experimental data is of great interest.

It was shown a few years ago [2] that it is possible to obtain the Wigner function of a mode of the electromagnetic field using a homodyne detection scheme. This scheme gives the probability distribution,  $P_\theta$ , of any quadrature component of the electromagnetic field. The Wigner function can be reconstructed from the probability distributions with the so-called inverse radon transform.

In quantum optics, this method has been applied so far only to the squeezed light obtained by parametric down-conversion [3,4]. Here, we present a new implementation of this method that enabled us to reconstruct for the first time the Wigner function of the field produced by the interaction of a laser beam with atoms placed in an optical cavity. The use of laser-cooled and -trapped atoms allows us to control the number of atoms so as to avoid spurious fluctuations.

Cold atoms constitute a very efficient non-linear medium and modify the quantum fluctuations to a large extent: it is possible to obtain noise reduction up to 40% in the absence of the trapping beams [5] or 55% conditional variance in a QND scheme [6]. In contrast to previous

---

(\*) Permanent address: Instituto de Física, Universidade Federal Fluminense, Av. Gal. Milton Tavares de Souza S/N Niterói, RJ 24210-340, Brasil.

(\*\*) Laboratoire de l'UPMC et de l'ENS, associé au CNRS.

experiments carried out with parametric generators, the state of the field obtained with cold atoms is not a minimum uncertainty one. In such cases, the Wigner function may bring more information than the one contained in the variances.

In our experimental scheme, the atoms are trapped by weak trapping beams and the beam having interacted with the atoms (probe beam) can show up to 22% noise reduction in good agreement with theoretical predictions [7]. Using cold trapped atoms and a set-up which is very stable against mechanical vibrations allows us to generate a state of light that does not change substantially over the course of the measurement. The probe field is detected by a standard homodyne detection which enables us to reconstruct its Wigner function through tomographic techniques. This procedure constitutes the so-called quantum tomography [2].

The electromagnetic field can be expressed in term of the rotated quadrature operators:

$$\hat{E}_{P, \theta} = \hat{E}_P \cos \theta + \hat{E}_Q \sin \theta, \quad \hat{E}_{Q, \theta} = -\hat{E}_P \sin \theta + \hat{E}_Q \cos \theta, \quad (1)$$

where  $\theta$  is an arbitrary phase.  $\hat{E}_P$  and  $\hat{E}_Q$  are the usual quadrature operators:

$$\hat{E}_P = \frac{1}{2} E_0 (\hat{a} + \hat{a}^\dagger), \quad \hat{E}_Q = \frac{i}{2} E_0 (\hat{a} - \hat{a}^\dagger), \quad (2)$$

where  $E_0$  is the field corresponding to one photon and  $\hat{a}$  and  $\hat{a}^\dagger$  are, respectively, the photon annihilation and creation operators.

The Wigner function,  $W(E_P, E_Q)$ , can be related to the probability distribution in a given quadrature component  $P_\theta(E_P, \theta)$  [2]:

$$P_\theta(E_P, \theta) = \int W(E_P, E_Q) dE_{Q, \theta}. \quad (3)$$

This relation can be inverted as

$$\begin{aligned} W(E_P, E_Q) &= \\ &= \int_{-\infty}^{+\infty} d\xi \int_{-\infty}^{+\infty} dk |k| \int_0^\pi d\theta P_\theta(\xi) \exp[2i\pi k (E_Q \cos \theta + E_P \sin \theta - \xi)]. \end{aligned} \quad (4)$$

A similar formula has been widely used in medical tomography to obtain images of the human body and is known as inverse radon transform. The numerical evaluation contains a filtering in phase space. To reduce the spurious effects of this filtering, we use a quadratic regularization method [8]. We rewrite the previous equation as

$$W(E_P, E_Q) = \int_0^\pi d\theta \int_{-\infty}^{+\infty} d\xi P_\theta(\xi) g(\xi - E_P, \theta), \quad (5)$$

where

$$g(x) = \int_{-\infty}^{+\infty} dk |k| \exp[-2i\pi kx]; \quad (6)$$

$g(x)$  can be replaced by  $g_\varepsilon(x)$ :

$$\begin{aligned} g_\varepsilon(x) &= \int_{-\infty}^{+\infty} dk |k| \exp[-4\pi^2 \varepsilon k^2 + 2i\pi kx] = \\ &= \frac{1}{\varepsilon} \left[ 1 - 2u \exp[-u^2] \int_0^u \exp[t^2] dt \right], \end{aligned} \quad (7)$$

with  $u = x/(2\sqrt{\varepsilon})$ . As  $\varepsilon$  goes to zero,  $g_\varepsilon$  converges to  $g$ .

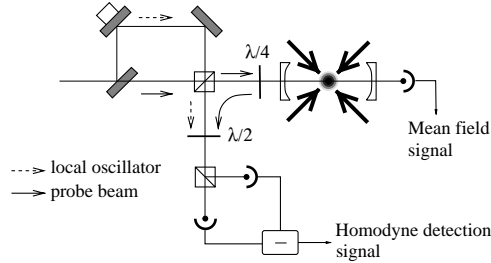


Fig. 1. – Experimental set-up for the measurement of the fluctuations.

It is also possible to reconstruct the photon number probability distribution using the method given in [9]. In this basis, a modification of the quantum fluctuations becomes apparent on the diagonal terms. For a vacuum state, the only non-zero term is  $\rho_{00}$ , while for squeezed vacuum states other non-zero terms exist. We have applied this reconstruction method to the field reflected by a cavity containing cold atoms.

Several papers have been devoted to the study of the noise reduction on a laser beam interacting with a set of two-level atoms placed in an optical cavity [10-12]. The cold atoms behave in a first approximation as a Kerr medium which is well known to produce bistable behaviour as well as noise reduction [13]. The use of laser-cooled atoms enables us to eliminate the Doppler broadening and thus to obtain a large non-linearity together with a small absorption.

In a previous experiment [5], the trap was switched off in order to reduce the excess noise due to the trapping beams. However, this scheme is not usable in a Wigner function measurement: as the trap is turned off, the atoms escape the interaction region resulting in a change of the optical length of the cavity over a few milliseconds. The tomographic measurement needs a large number of points to be recorded (500.000 in our case) which takes 1 s using our data acquisition system. Thus, the trapping beams must be turned on during the whole measurement. In order to reduce their spurious noise, their power must be kept low (below 1 mW). To determine the optimum working conditions, we have developed a three-level model for the atomic medium which is described in ref. [7]. In the optimum configuration, the observed noise reduction is around 22% over several seconds.

The experimental set-up is described in detail in [7]. The cold atoms are prepared using a standard magneto-optical trap in which three orthogonal circularly polarized trapping beams are generated by a Ti:Sapphire laser. The trapping beams are detuned to the low-frequency side of the  $6S_{1/2}F = 4$  to  $6P_{3/2}F = 5$  transition. As usual, to prevent atoms from being optically pumped to the  $6S_{1/2}F = 3$  state, we superimpose a diode laser tuned to the  $6S_{1/2}F = 3$  to  $6P_{3/2}F = 4$  transition to the trapping beams.

We use a 25 cm long linear cavity close to the hemifocal configuration with a waist of  $260 \mu\text{m}$  (fig. 1). The transmission of the coupling mirror is 10% while the end mirror is highly reflecting. Thus, the cavity is close to the “bad cavity” case, where the linewidth of the cavity (5 MHz) is of the same order of or larger than the atomic linewidth (2.6 MHz). We send a circularly polarized probe beam inside the cavity. The frequency of the probe is detuned by 50 MHz on the low-frequency side of the  $6S_{1/2}F = 4$  to  $6P_{3/2}F = 5$  transition. The power of the probe beam is of the order of  $7 \mu\text{W}$  and its coupling efficiency to the cavity mode is over 97%. We can measure the power of the probe beam transmitted through the cavity with a photodiode located behind the end mirror. This intensity can be compared to a fixed level and the error signal thus obtained is sent to a piezo-electric ceramic attached to this mirror. This enables us to control the length of the cavity.

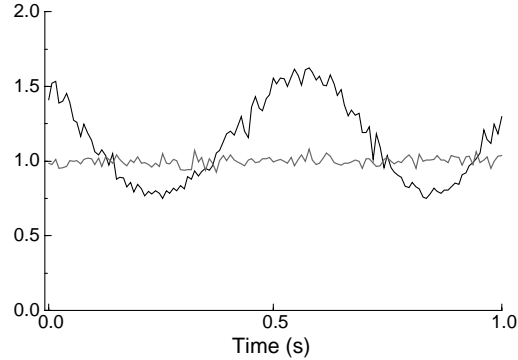


Fig. 2. – Evolution of the variance of the homodyne detection signal used for the reconstruction as the local oscillator phase is swept.

The field reflected from the cavity is separated by an optical circulator consisting of a quarter wave plate and a polarizing beamsplitter. To achieve the homodyne detection, the probe beam is mixed with a powerful local oscillator using the second input port of the beamsplitter. The ratio of the intensities of the probe and the OLO is on the order of 1:1000. The phase of the OLO can be scanned using a mirror mounted on a piezo-electric ceramic. We use a half-wave plate and a second polarizing beamsplitter to split the two fields which are then detected by highly efficient photodiodes (87% quantum efficiency). The total detection efficiency is around 85%. Electronic noise is 8 dB below the shot noise level.

The AC parts of the photodiodes are subtracted and amplified to form the homodyne detection signal. This signal is mixed with an electronic local oscillator (ELO) at 8 MHz which is in the optimum frequency range for squeezing [7]. The signal is then filtered with a bandwidth of 100 kHz and amplified to detect the noise component at the ELO's frequency. Filtering prevents averaging over different noise frequencies which have different noise values. We digitize the signal using a AT-MIO 16E2 data acquisition card from National Instruments with a maximum sampling rate of 500 kHz.

To record data, the cavity is set at a given length and we scan the phase of the OLO. We record 500000 data points during one second corresponding to a variation of the phase of the local oscillator of the order of  $\pi$ . We then divide this ensemble into 128 data sets and assign a fixed phase to each set. The marginal distributions correspond to the number of counts in 128 different amplitude bins. Using these marginal distributions, the Wigner function is calculated with the quadratic filtering algorithm.

From these marginal distributions, we have first calculated the variance of the homodyne detection signal (fig. 2). The oscillations show the variation of the noise as a function of the phase of the OLO. The value 1 corresponds to the shot-noise level and the figure clearly shows that the noise is reduced below this limit by 22%.

The Wigner function is fitted by a 3-dimensional Gaussian. A Gaussian shape is expected for the Wigner function in this case, since the fluctuations are small compared to the mean value [14]. The fitting function is given by the equation

$$f(E_P, E_Q) = z_M \exp \left[ - \left( \frac{E_{P,\theta} - E_P^0}{a} \right)^2 - \left( \frac{E_{Q,\theta} - E_Q^0}{b} \right)^2 \right]. \quad (8)$$

The agreement between the fitted function and the experimental data given by a  $\chi^2$  statistical

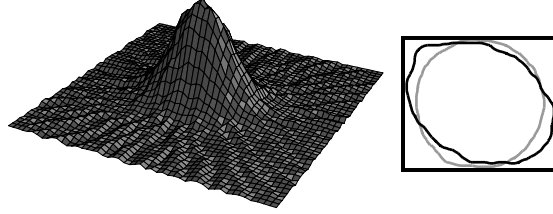


Fig. 3. – 3D view of the Wigner function for a squeezed state (left), sections of the Wigner function for a coherent state (grey curve) and for a squeezed state (black curve) (right).

test is satisfactory. The widths of the Gaussian,  $a$  and  $b$ , can be related to the optimum squeezing,  $S_{\min}$  and maximum excess noise,  $S_{\max}$ .  $S_{\min}$  and  $S_{\max}$  can be compared to the measurement made previously or performed with a spectrum analyser. The values obtained by these different methods are in good agreement.

In the case of the vacuum state, the fitted function,  $f(E_P, E_Q)$ , obtained in the experiment with no probe beam, exhibits a circular symmetry which can be seen on the section at  $1/e$  of the maximum (grey curve on the right of fig. 3). This is expected theoretically since there is no preferred quadrature. In the case of a squeezed state, the corresponding section is an ellipse (black curve on the right of fig. 3). The large axis corresponds to excess noise while the small axis corresponds to noise reduction.

We have also reconstructed the photon number probability distribution (fig. 4). As expected, the only non-zero term for the vacuum state is found to be  $\rho_{00}$  (fig. 4, left). For the squeezed state, the distribution is broader (fig. 4, center). It is also possible to calculate the photon number probability distribution by assuming that the Wigner function is Gaussian. The minimum and maximum widths at  $1/e$  are given by the minimum and maximum variances of the homodyne detection signal. The agreement between the experimentally reconstructed and the calculated photon number probabilities is very good.

Yet, our experimental data does not show zero values for odd terms. To investigate this, we have calculated the photon number distribution for a minimum uncertainty state with a squeezing of 22% detected with a detection efficiency of 85% (fig. 4, right, curve (c)) and with a perfect detection (fig. 4, right, curve (d)). The minimum uncertainty state exhibits a

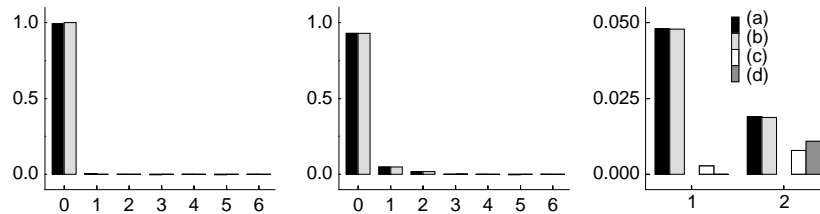


Fig. 4. – Photon number distribution for shot-noise (left) and for a squeezed state (center). The diagram on the right is an enlargement of the photon number distributions for 1 and 2 photons ( $\rho_{11}$  and  $\rho_{22}$ ), computed in four cases:  $\rho_{11}$  and  $\rho_{22}$  obtained (a) from the probability distributions, (b) from a calculation assuming a Gaussian Wigner function with the measured value of noise reduction and excess noise, (c) from a calculation assuming a minimum uncertainty state with our value of noise reduction and imperfect detection, (d) from a calculation assuming a minimum uncertainty state with our value of noise reduction and perfect detection.

zero probability value for odd photon number terms, as expected. However, the value of  $\rho_{11}$  becomes non-zero as soon as the detection is non-perfect. On the other hand, a squeezed state with our values of noise reduction and excess noise has  $\rho_{11}$  greater than  $\rho_{22}$  even with a perfect detection. Thus, the fact that  $\rho_{11}$  is non-zero comes from non-perfect detection efficiency as well as from the fact that the state is not minimal.

In conclusion, we have used the method of quantum tomography to reconstruct the Wigner function of a laser beam having interacted with a cloud of cold atoms placed in an optical cavity. The Wigner function exhibits non-classical features, one of its quadrature having fluctuations below the standard quantum limit. This measurement of the field emitted by an atomic cloud opens the way to the investigation of systems containing small numbers of atoms for which the Wigner function is predicted to have a non-Gaussian character.

#### REFERENCES

- [1] WIGNER E. P., *Phys. Rev.*, **40** (1932) 749.
- [2] VOGEL K. and RISKEN H., *Phys. Rev. A*, **40** (1989) 2847.
- [3] SMITHEY D. T., BECK M., RAYMER M. G. and FARIDANI A., *Phys. Rev. Lett.*, **70** (1993) 1244.
- [4] BREITENBACH G., SCHILLER S. and MLYNEK J., *Nature*, **387** (1997) 471.
- [5] LAMBRECHT A., COUDREAU T., STEINBERG A. M. and GIACOBINO E., *Europhys. Lett.*, **36** (1996) 93.
- [6] ROCH J. F., VIGNERON K., GRELU PH., SINATRA A., POIZAT J. PH. and GRANGIER PH., *Phys. Rev. Lett.*, **78** (1997) 644.
- [7] KHOURY A. Z., COUDREAU T., FABRE C. and GIACOBINO E., *Phys. Rev. A*, **57** (1998) 4770.
- [8] JANICKE U. and WILKENS M., *J. Mod. Opt.*, **42** (1995) 2183.
- [9] LEONHARDT U., MUNROE M., KISS T., RICHTER T. H. and RAYMER M. G., *Opt. Commun.*, **127** (1996) 144.
- [10] HILICO L., FABRE C., REYNAUD S. and GIACOBINO E., *Phys. Rev. A*, **46** (1992) 4397.
- [11] REID M. D., *Phys. Rev. A*, **37** (1988) 4792.
- [12] CASTELLI F., LUGIATO L. A. and VADACCHINO M., *Nuovo Cimento D*, **10** (1988) 183.
- [13] REYNAUD S., FABRE C., GIACOBINO E. and HEIDMANN A., *Phys. Rev. A*, **40** (1989) 1440.
- [14] EKERT A. K. and KNIGHT P. L., *Phys. Rev. A*, **43** (1991) 3934.